



Available online at www.sciencedirect.com

## **ScienceDirect**

Advances in Space Research 69 (2022) 2951-2956

ADVANCES IN SPACE RESEARCH (a COSPAR publication)

www.elsevier.com/locate/asr

# The effect of F10.7 on interhemispheric differences in ionospheric current during solstices

Tre'Shunda James\*, Ramon E. Lopez

Department of Physics, The University of Texas at Arlington, Arlington, TX 76019, USA

Received 20 October 2021; received in revised form 17 January 2022; accepted 5 February 2022

Available online 11 February 2022

#### Abstract

We investigate the differences in the electrojet and Birkeland current systems during summer and winter solstice and the effect of F10.7. The difference in solar illumination of the polar ionosphere during the winter versus summer solstice results in significantly higher conductivity in the summer polar ionosphere. As expected, the currents are larger during the summer than during the winter. The relationship between the electrojets and the Birkeland current systems is essentially constant across seasons, as expected if the ionospheric electrojets close the Birkeland currents. The magnitude of F10.7 is an indicator of the level of solar-generated ionospheric conductance, therefore, one would expect larger ionospheric currents during periods of larger F10.7. This holds true for the summer solstice periods, however, the opposite trend is observed during the winter solstice periods. We provide an explanation for this finding based on the control of the dayside merging rate by the magnetosheath flow pattern.

© 2022 COSPAR. Published by Elsevier B.V. This is an open access article under the CC BY-NC-ND license (http://creativecommons.org/licenses/by-nc-nd/4.0/).

Keywords: Birkeland current; Ionospheric conductivity; Geoeffective length; Ionospheric conductance; Ionospheric potential

#### 1. Introduction

Large-scale field-aligned currents couple the magnetosphere to the ionosphere. These currents, known as Birkeland currents, consist of two current systems that can be differentiated by latitude and the direction in which they flow into Earth's polar region depending on the local time (Iijima and Potemra, 1976). The Region 1 Birkeland currents flow into the ionosphere at dawn and out of the ionosphere at dusk at high latitudes near the open-closed field line boundary. This current transmits solar wind stress to the ionosphere, and its magnitude depends on the amount of solar wind-magnetosphere coupling (Lopez et al., 2010; Lopez, 2016), which is primarily the result of merging between the IMF and the geomagnetic field. There is an additional energy transfer mechanism, the viscous interac-

tion (Bruntz et al., 2012) that also drives Region 1 currents (at somewhat lower latitudes). However, the primary mechanism for the transfer of the energy and momentum from the solar wind to the magnetosphere-ionosphere system is driven by the merging interaction (Newell et al., 2008). The merging interaction under most conditions can be considered to be proportional to the solar wind electric field, but under conditions of low solar wind Mach number, the dayside merging rate saturates (Borovsky and Birn, 2014; Lavraud and Borovsky, 2008; Lopez et al., 2010; Lopez, 2016). Under these conditions the correlations between ionospheric currents and the typical solar wind coupling functions are weaker (McPherron et al., 2015).

The Region 2 Birkeland currents are driven by plasma pressure gradients in the inner magnetosphere, they flow in the opposite polarity to Region 1, and are found at lower latitudes than the former (e.g., Ganushkina et al., 2018). The Birkeland currents close through the auroral electrojet,

<sup>\*</sup> Corresponding author.

E-mail address: tresunda.james@mavs.uta.edu (T. James).

which is the horizontal current in the auroral region of the ionosphere. The magnitude of the electrojets are indexed by finding the largest northward or southward perturbation from ground magnetometers. The largest observed northward perturbation in nT, which is positive in the HDZ coordinate system, is an indicator of the largest eastward electrojet and is called AU. The largest observed southward perturbation in nT, which is negative in the HDZ coordinate system, is an indicator of the largest westward electrojet and is called AL. The AE index is defined as AU minus AL, and it is a measure of the global level of activity of the electrojets (Davis and Sugiura, 1966).

Given a certain ionospheric potential produced by the interaction of the solar wind with the geospace system, currents will flow with the magnitude of the current depending on the ionospheric conductivity. Ionospheric conductivity is driven in part by solar extreme ultraviolet (EUV) radiation (Ridley et al., 2004). Solar ultraviolet radiation is dependent on solar zenith angle and the level of electromagnetic radiation produced by the Sun, which is typically quantified using the F10.7 index. Increased solar illumination increases ionospheric conductivity, in which, in return, increases the intensity of Region 1 currents (Fujii and Iijima, 1987). The horizontal ionospheric currents also depend on the solar illumination. Ohtani et al. (2019) found that the magnitude of the dayside electrojets where controlled by the solar zenith angle, while the nightside electrojets also included a dependence on the dipole tilt angle. However, as seasons change the amount of EUV radiation seen by Earth's polar cap varies drastically. During the summer, the northern polar cap is entirely illuminated, but during the winter this same region receives almost no sunlight; and because EUV provides the baseline conductivity of the ionosphere, the currents flowing in the ionosphere exhibits a seasonal asymmetry.

Previous work has quantified this seasonal asymmetry in terms of the magnitude of the Birkeland currents (e.g., Juusola et al., 2009; Papitashvili et al., 2002; Ohtani et al., 2005). Juusola et al. (2009) reported the Birkeland current in the summer to be 1.4 times larger than that in the winter, which is also well within the range of the 1.35 ratio reported by Papitashvili et al. (2002). Similarly, Weimer et al. (1990) investigated the seasonal variation of AE and the relationship to the ionospheric potential. However, no work has yet quantified the seasonal asymmetry of electrojet magnitude using SME (SuperMag Electrojet, see Gjerloev (2012)) which is a more global measure than the AE index. In this work we do just that. Moreover, we investigate the correlation between SME and the total Birkeland current, and the variation of these quantities with F10.7.

#### 2. Data and observations

We conduct this study of the seasonal asymmetry in ionospheric current using SME as a measure of the strength of the auroral electrojets and the Birkeland cur-

rents in the northern hemisphere using data from **AMPERE** (http://ampere.jhuapl.edu/products/itot/). AMPERE collects data from the Iridium satellite system. which comprise over 70 satellites, each equipped with a magnetometer. The magnetic field data provides global maps of Birkeland currents (Anderson et al., 2000). The data used in this study span the years of 2010–2017, excluding the years associated with AMPERE data gaps, and are centered on the weeks of the summer and winter solstices to maximize the difference in solar illumination. The summer solstice weeks used were June 18-24 for years 2010-2013 and 2015–2017, while the winter solstice weeks used were December 18-24 2010-2013 and 2015-2016. Moreover, since we average over the entire week, the dipole tilt angle dependence of the nightside electrojets discussed by Ohtani et al. (2019) should average out, leaving just the solar EUV dependence. We use the SME index data from SuperMag (http://supermag.jhuapl.edu/indices/), which is derived from approximately 110 ground-based magnetometers stations. The SMU index represents the eastward electrojet (and corresponds to AU), while the SML index represents the westward electrojet (and corresponds to AL). SME is the difference between SMU and SML, just as AE is the difference between AU and AL. We use the SME index instead of AE, because it is derived from many more stations, allowing for a more accurate global measure.

To quantify the driver of the SME index, we use the solar wind electric field from the OMNI data set. We obtained the OMNI data from CDAWeb (https://cdaweb.gsfc.nasa.gov/pub/data/omni/high res omni/monthly\_1min/). The data are taken the 1-week periods centered on the winter and summer solstices and are binned by solar wind electric field (0.4 mV/m intervals of southward IMF), except for the largest values of the solar wind electric field where there are a smaller number of points. Those were put into a single bin. The Birkeland current data from the AMPERE website and the solar wind data were averaged over 1 h. The solar wind data have not been lagged relative to the SME and Birkeland current data. We did examine if shifting the solar wind data by 5 or 10 min relative to the other data sets made a difference, but we found essentially no change in the results to be presented here.

The integrated dayside reconnection rate, which is a measure of the energy transfer from the solar wind to the magnetosphere, is proportional to the solar wind electric field for magnetosonic Mach number > 4 (Lopez, 2016). Therefore, we plot SME vs Electric Field (Fig. 1). Upon visual inspection, it is evident that the average value of the SME index in the summer is higher than that in the winter. On average, taking the summer-winter ratio in each bin, the average SME index in the summer is approximately 1.4 times greater than it is in the winter.

The Birkeland current exhibits the same behavior as the SME index as a function of solar wind electric field. The last bin is a cumulative bin including periods when the day-side merging rate is saturated (Lopez et al., 2010). When

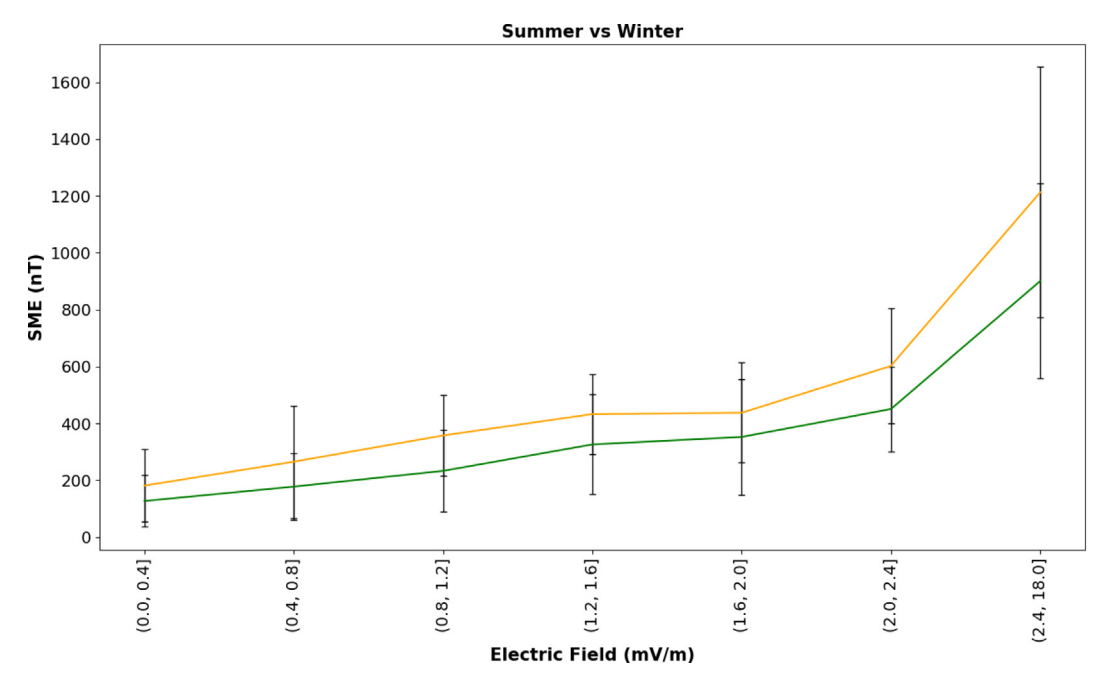


Fig. 1. SME vs Solar Wind Electric Field. The weeks centered on the summer solstice are plotted in yellow. The green data are for the weeks centered on the winter solstice. The electric field is binned in 0.04 mV/m increments, except for the last bin in which the Mach number is low and the current has saturated.

saturation occurs, the dayside merging rate (and thus the ionospheric potential) becomes insensitive to the magnitude of the solar wind electric field and depends on other factors, such as solar wind density. We find that the summer-winter ratio of the Birkeland current magnitude under unsaturated conditions is about 1.6 (Fig. 2).

We have also correlated the relationship between the SME index and the Birkeland current across season, pre-

sented in Fig. 3. We only use data with SME values less that 750 nT to avoid extremely active periods when factors like saturation of the ionospheric potential could complicate the relationships (McPherron et al., 2015) or sudden extreme values of the SME index or the Birkeland currents could produce outlier points that unduly influence the linear fits. The slopes of the linear fits for the SME index as a function of the Birkeland current fall within each others

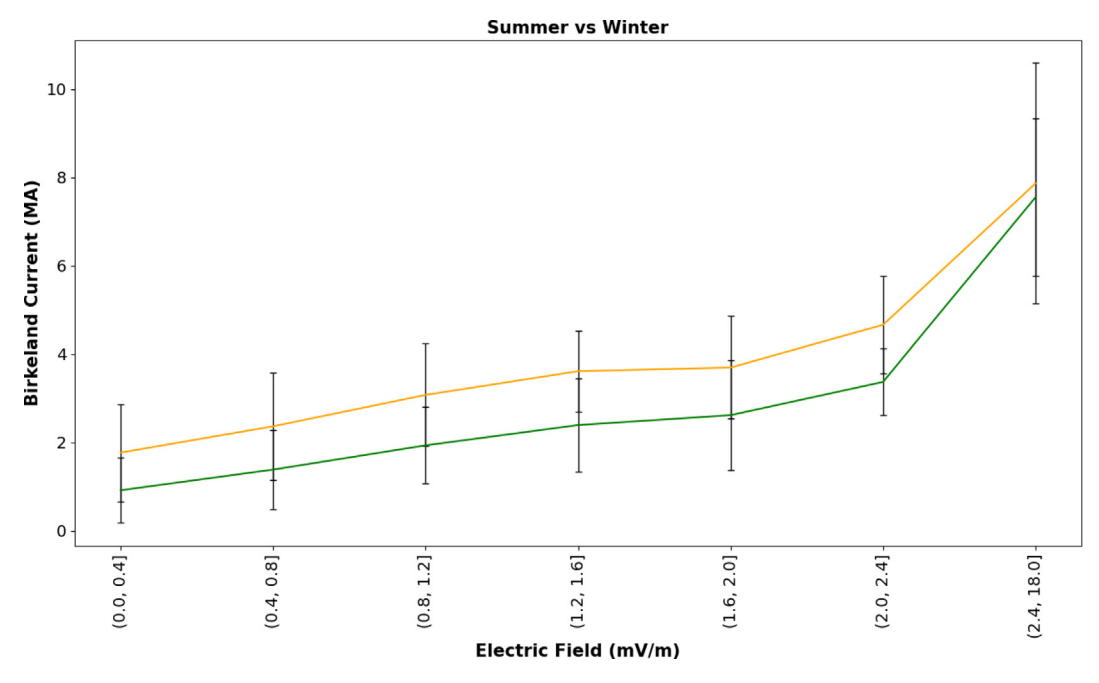


Fig. 2. Birkeland Current vs Solar Wind Electric Field. The data are binned in 0.4 mV/m increments, except for the last bin. In yellow are the data for the summer weeks and the green are the data for the winter weeks.

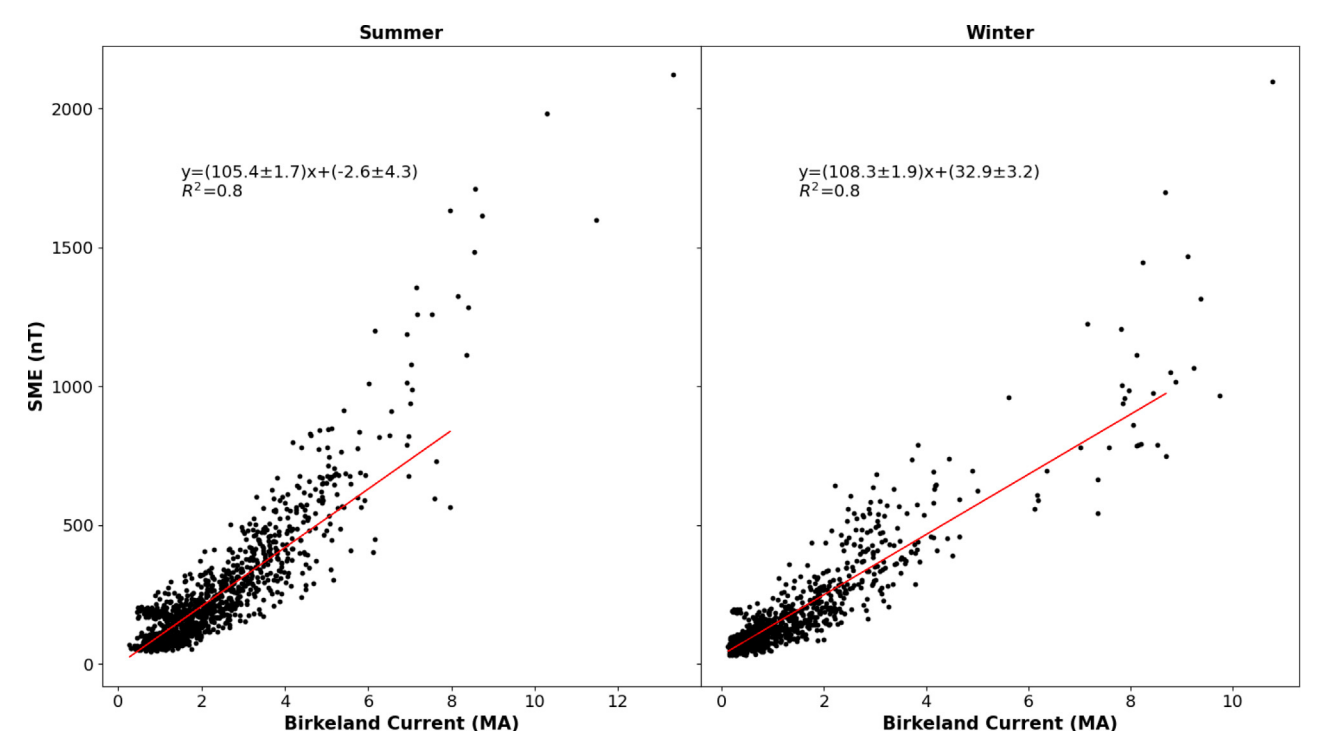


Fig. 3. The relationship between SME and total Birkeland Current for weeks centered on the summer solstice (left) and weeks centered on the winter solstice (right).

error bars. This means that the relationship between the SME index and Birkeland Current is essentially independent of ionospheric conductivity, as it should if there is one big current system in which the eastward and westward electrojets close the Birkeland currents.

Additionally, we investigated the dependence of the magnitude of the currents on the value of the F10.7 index. Because the F10.7 index is a proxy for the solar EUV flux, we expect greater F10.7 to correlate with greater ionospheric conductivity and larger values of the currents for a given solar wind electric field. The summer and winter solstice weeks data for the lowest electric field bin (0.0 mV/m-0.4 mV/m) were separated into 3 bins of F10.7: an overall average bin, a high bin (top third of F10.7 values), and a low bin (bottom third of F10.7 values). We find that, as expected, during the summer solstice weeks the value of the SME index and the total Birkeland current increased with F10.7. However, the opposite trend was observed during the winter solstice weeks; higher F10.7 is correlated with lower values of both the SME index and the total Birkeland current(Table 1). Other solar wind electric field bins (which have fewer points) exhibit the same trend. This is a surprising and seemingly counter-intuitive result.

#### 3. Findings and discussion

This work has demonstrated quantitatively that the average total Birkeland current and the average SME are larger in the summer than in the winter. These results are

in agreement with previous studies. Also, we have quantitatively found a consistent correlation between the SME and Birkeland current for both summer and winter solstice periods, so that relationship is independent of ionospheric conductivity. This finding is consistent with the idea that the Birkeland currents are closed via the eastward and westward electrojets. The relationship between the current flowing through the polar ionosphere and the F10.7 index for the summer solstice weeks follows the expected pattern. For larger F10.7, hence large ionospheric conductivity, the larger the current for a given solar wind electric field. However, for the winter solstice period, this relationship is reversed, with a larger F10.7 correlated with a smaller net current flowing through the ionosphere. To explain this result, we must consider how the voltage across the polar cap is generated in the first place, and the effect of ionospheric conductivity on that voltage.

The Force Balance Model for the generation of the ionospheric potential due to reconnection explains how ionospheric conductivity controls the portion of the transpolar potential generated by merging (Lopez et al., 2010). For identical solar wind conditions, the Region 1 currents are larger for a higher ionospheric conductivity. Larger Region 1 currents cause greater magnetopause erosion (e.g., Wiltberger et al., 2003). Thus, the magnetopause at noon is closer to the Earth for higher levels of ionospheric conductivity compared to lower levels. This can be seen in simulation results taken from Lopez et al. (2010) and presented in Fig. 4 in which the magnetopause was about 0.9 times closer to Earth (about 8 vs. 9 Earth radii) and the

Table 1 F10.7 Variance.<sup>a</sup>

Number of Hours (total, high, low)	Avg. SME [nT] (total, high, low)	Avg. Birkeland Current [MA] (total, high, low)	Avg. Solar Wind Electric Field [mV/m]	Avg. F10.7 (total, high, low)
203	182.9	1.8		96
67	214.3	2.0	0.2	127.0
67	136.4	1.5		75.2
189	127.2	0.9		107.8
63	108.4	0.8	0.2	137.4
63	147.1	1.1		74.0

<sup>&</sup>lt;sup>a</sup> The top three rows of data are for the summer and the bottom three rows of data are for the winter.

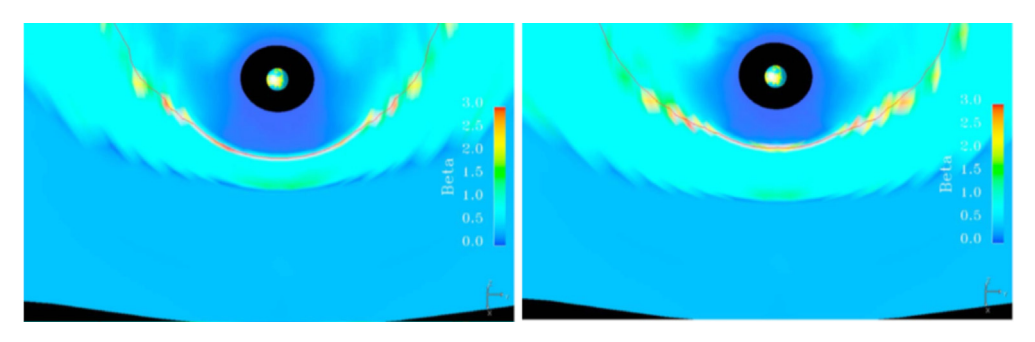


Fig. 4. The panels are generated by a global magnetosphere simulation (Lopez et al., 2010). This figure displays the position of the magnetopause (black line) with a conductivity of 5 mho (left) and 10 mho (right) for identical solar wind conditions with southward IMF.

ionospheric potential was 0.6 times lower (150 kV versus 250 kV) for the higher conductivity case. Observations have confirmed the relationship between magnetopause erosion using the F10.7 index as a proxy for ionospheric conductivity, with larger F10.7 correlated with a more eroded magnetopause (Němeček et al., 2016).

The magnetosheath plasma flow pattern will be modified by this change of shape of the magnetopause. For the higher ionospheric conductivity case, the magnetosphere is blunter, the stagnation of the flow is greater and less magnetic flux will reach the dayside merging line. In other words, the geoeffective length (the y-extent of the solar wind flow that reaches the merging line) gets smaller. The lower dayside merging rate results in a lower ionospheric potential, which is the sum of the potential due to reconnection and the (smaller) potential due to the viscous interaction (Lopez et al., 2010), as seen in the simulation results. Thus, a system with a larger ionospheric conductivity will have a larger total Region 1 current, but a smaller dayside merging rate and so a smaller total ionospheric potential. Since the Region 1 current in the more conducting ionosphere is larger (despite the smaller total ionospheric potential), the electrojet currents closing the Birkeland currents will also be larger.

Now consider the case in which the baseline ionospheric conductivities are not the same in the two hemispheres. The hemisphere with the larger conductivity will have the largest Region 1 flowing through it, and it will control the amount of magnetopause erosion and the geoeffective length, which sets the value of the portion of the ionospheric potential due to reconnection. Now consider the situation at sol-

stice. The sunlit hemisphere has the higher conductivity and so it controls the overall value of the potential. If the value of F10.7 is larger than average, the sunlit hemisphere is more conducting than average, the Region 1 current is larger than average and the potential from reconnection is lower than average due to a smaller geoeffective length. Since the potential produced by reconnection must be the same in both hemispheres (because the amount of open flux and the changes in that flux must be the same in both hemispheres), the potential in both polar caps decreases as F10.7 due to the change in the geoeffective length. In the summer polar cap. the increasing F10.7 corresponds to an increase in ionospheric conductivity and an increase in both the total Birkeland current and the electrojet currents, despite the fact that the ionospheric potential decreases. This leads to the correlations between currents and F10.7 seen in the summer solstice weeks. In the dark polar cap, increasing F10.7 does not increase conductivity because the dark region is not illuminated. Therefore, with an unchanged conductivity but a smaller ionospheric potential, the current in the dark hemisphere is reduced as F10.7 increases. Thus our seemingly contradictory result of the current decreasing in the winter solstice hemisphere with increasing F10.7 is actually a direct consequence of the force balance model prediction of the change in the geoeffective length with increasing conductivity.

#### 4. Conclusions

We have examined the relationships between the total Birkeland current and the SME index in the northern hemisphere as a function of solar wind electric field, season, and

F10.7. In agreement with previous studies, we find that the current flowing regardless of season increases with increasing solar wind electric field (for high solar wind Mach number), and the total current during summer solstice is about 40% larger than the current during winter solstice due to the higher conductivity in the sunlit hemisphere. The relationship between the amount of Birkeland current and the SME index is essentially the same during summer and winter solstice periods. This indicates that the relationship is not dependent on ionospheric conductivity. Instead, the correlations is consistent with current continuity and the Birkeland currents being closed via the auroral electrojets. The relationship between F10.7 and the total current is consistent with the conductivity hypothesis for the summer solstice periods: larger values of F10.7 (larger ionospheric conductivity) are correlated with larger currents for a given solar wind electric field. This relationship is reversed during winter solstice, with high values of F10.7 being correlated with lower values of current for a given solar wind electric field. This result is a natural consequence of the Force Balance Model for the ionospheric potential and it provides additional strong support for that model.

#### **Declaration of Competing Interest**

The authors declare that they have no known competing financial interests or personal relationships that could have appeared to influence the work reported in this paper.

### Acknowledgments

We gratefully acknowledge the SuperMAG website and the data there provided by SuperMAG collaborators. The SME data can be found at http://supermag.jhuapl.edu/ indices for the periods described in the paper. We thank the AMPERE team and the AMPERE Science Center for providing the Iridium derived data products. The AMPERE Birkeland current data can be found at http:// ampere.jhuapl.edu/products/itot/daily.html for each day at 2-min time resolution. We acknowledge the use of the OMNI data set, which were obtained from CDAWeb using the Space Physics Data Facility(SPDF) https://cdaweb. gsfc.nasa.gov/pub/data/omni/high res omni/monthly 1min/. We acknowledge the support of the US National Science Foundation (NSF) under Grant No. 1916604. We also acknowledge the support of The National Aeronautics and Space Administration (NASA) under Grant No. 80NSSC20K0606 (The Center for the Unified Study of Interhemispheric Asymmetries (CUSIA)) and Grant No. 80NSSC21K2057.

#### References

- Anderson, B.J., Takahashi, K., Toth, B.A., 2000. Sensing global birkeland currents with iridium engineering magnetometer data. Geophys. Res. Lett. 27 (24), 4045–4048.
- Borovsky, J.E., Birn, J., 2014. The solar wind electric field does not control the dayside reconnection rate. J. Geophys. Res.: Space Phys. 119 (2), 751–760.
- Bruntz, R., Lopez, R., Wiltberger, M., Lyon, J., 2012. Investigation of the viscous potential using an mhd simulation. J. Geophys. Res.: Space Phys. 117 (A3).
- Davis, T.N., Sugiura, M., 1966. Auroral electrojet activity index ae and its universal time variations. J. Geophys. Res. 71 (3), 785–801.
- Fujii, R., Iijima, T., 1987. Control of the ionospheric conductivities on large-scale birkeland current intensities under geomagnetic quiet conditions. J. Geophys. Res.: Space Phys. 92 (A5), 4505–4513.
- Ganushkina, N.Y., Liemohn, M., Dubyagin, S., 2018. Current systems in the earth's magnetosphere. Rev. Geophys. 56 (2), 309–332.
- Gjerloev, J., 2012. The supermag data processing technique. J. Geophys. Res.: Space Phys. 117 (A9).
- Iijima, T., Potemra, T.A., 1976. Field-aligned currents in the dayside cusp observed by triad. J. Geophys. Res. 81 (34), 5971–5979.
- Juusola, L., Kauristie, K., Amm, O., Ritter, P., 2009. Statistical dependence of auroral ionospheric currents on solar wind and geomagnetic parameters from 5 years of champ satellite data. Annales Geophysicae, vol. 27. Copernicus GmbH, pp. 1005–1017.
- Lavraud, B., Borovsky, J.E., 2008. Altered solar wind-magnetosphere interaction at low mach numbers: Coronal mass ejections. J. Geophys. Res.: Space Phys. 113 (A9).
- Lopez, R., Bruntz, R., Mitchell, E., Wiltberger, M., Lyon, J., Merkin, V., 2010. Role of magnetosheath force balance in regulating the dayside reconnection potential. J. Geophys. Res.: Space Phys. 115 (A12).
- Lopez, R.E., 2016. The integrated dayside merging rate is controlled primarily by the solar wind. J. Geophys. Res.: Space Phys. 121 (5), 4435-4445
- McPherron, R.L., Hsu, T.-S., Chu, X., 2015. An optimum solar wind coupling function for the al index. J. Geophys. Res.: Space Phys. 120 (4), 2494–2515.
- Němeček, Z., Šafránková, J., Lopez, R., Dušík, Š., Nouzák, L., Přech, L., Šimnek, J., Shue, J.-H., 2016. Solar cycle variations of magnetopause locations. Adv. Space Res. 58 (2), 240–248.
- Newell, P.T., Sotirelis, T., Liou, K., Rich, F., 2008. Pairs of solar wind-magnetosphere coupling functions: Combining a merging term with a viscous term works best. J. Geophys. Res.: Space Phys. 113 (A4).
- Ohtani, S., Gjerloev, J.W., Johnsen, M.G., Yamauchi, M., Brändström, U., Lewis, A.M., 2019. Solar illumination dependence of the auroral electrojet intensity: Interplay between the solar zenith angle and dipole tilt. J. Geophys. Res.: Space Phys. 124 (8), 6636–6653.
- Ohtani, S., Ueno, G., Higuchi, T., 2005. Comparison of large-scale field-aligned currents under sunlit and dark ionospheric conditions. J. Geophys. Res.: Space Phys. 110 (A9).
- Papitashvili, V., Christiansen, F., Neubert, T., 2002. A new model of field-aligned currents derived from high-precision satellite magnetic field data. Geophys. Res. Lett. 29 (14), 28–1.
- Ridley, A., Gombosi, T.I., DeZeeuw, D., 2004. Ionospheric control of the magnetosphere: Conductance. Annales Geophysicae, vol. 22. Copernicus GmbH, pp. 567–584.
- Weimer, D., Maynard, N., Burke, W., Liebrecht, C., 1990. Polar cap potentials and the auroral electrojet indices. Planet. Space Sci. 38 (9), 1207–1222.
- Wiltberger, M., Lopez, R., Lyon, J., 2003. Magnetopause erosion: A global view from mhd simulation. J. Geophys. Res.: Space Phys. 108 (A6)